

Endurance of SN 2005ip after a decade: X-rays, radio, and H α like SN 1988Z require long-lived pre-supernova mass loss

Nathan Smith^{1*}, Charles D. Kilpatrick¹, Jon C. Mauerhan², Jennifer E. Andrews¹, Raffaella Margutti^{3,4}, Wen-Fai Fong^{1,5}, Melissa L. Graham^{2,6}, WeiKang Zheng², Patrick L. Kelly², Alexei V. Filippenko², Ori D. Fox⁷

¹Steward Observatory, University of Arizona, Tucson, AZ 85721, USA

²Department of Astronomy, University of California, Berkeley, CA 94720-3411, USA

³Center for Interdisciplinary Exploration and Research in Astrophysics (CIERA), and Department of Physics and Astrophysics, Northwestern University, Evanston, IL 60208, USA

⁴Center for Cosmology and Particle Physics, New York University, 4 Washington Place, New York, NY 10003, USA

⁵Einstein Fellow

⁶Department of Astronomy, University of Washington, Box 351580, Seattle, WA 98195-1580, USA

⁷Space Telescope Science Institute, 3700 San Martin Drive, Baltimore, MD 21218, USA

Accepted 0000, Received 0000, in original form 0000

ABSTRACT

Supernova (SN) 2005ip was a Type IIn event notable for its sustained strong interaction with circumstellar material (CSM), coronal emission lines, and infrared (IR) excess, interpreted as shock interaction with the very dense and clumpy wind of an extreme red supergiant. We present a series of late-time spectra of SN 2005ip and a first radio detection of this SN, plus late-time X-rays, all of which indicate that its CSM interaction is still strong a decade post-explosion. We also present and discuss new spectra of geriatric SNe with continued CSM interaction: SN 1988Z, SN 1993J, and SN 1998S. From 3–10 yr post-explosion, SN 2005ip’s H α luminosity and other observed characteristics were nearly identical to those of the radio-luminous SN 1988Z, and much more luminous than SNe 1993J and 1998S. At 10 yr after explosion, SN 2005ip showed a drop in H α luminosity, followed by a quick resurgence over several months. We interpret this H α variability as ejecta crashing into a dense shell located $\lesssim 0.05$ pc from the star, which may be the same shell that caused the IR echo at earlier epochs. The extreme H α luminosities in SN 2005ip and SN 1988Z are still dominated by the forward shock at 10 yr post-explosion, whereas SN 1993J and SN 1998S are dominated by the reverse shock at a similar age. Continuous strong CSM interaction in SNe 2005ip and 1988Z is indicative of enhanced mass loss for $\sim 10^3$ yr before core collapse, longer than Ne, O, or Si burning phases. Instead, the episodic mass loss must extend back through C burning and perhaps even part of He burning.

Key words: circumstellar matter — stars: evolution — stars: winds, outflows — supernovae: general — supernovae: individual (SN 2005ip)

1 INTRODUCTION

Type IIn supernovae (SNe IIn) have raised important questions about the latest phases of evolution in massive stars, because they require enhanced or episodic mass loss shortly before core collapse that far exceeds known examples of steady winds (see Smith 2014 for a general review of mass loss and its connection to interacting SNe). SNe IIn have relatively narrow lines of hydrogen in their spectra (see Filippenko 1997 for a review of SN spectral classification) caused by slow-moving circumstellar material (CSM) that

is hit by the blast wave or illuminated by ultraviolet (UV) radiation from the SN. In some extreme cases, as much as 10–25 M \odot seems to have been ejected in just the decade before core collapse (Smith et al. 2007; Woosley et al. 2007; Smith et al. 2008a, 2010; Ofek et al. 2014). In other cases, the luminosity enhancement is more modest, but the CSM is still dense enough to correspond to the strongest known winds from extreme and unstable red supergiants (RSGs; e.g., Smith et al. 2009b). SNe IIn are about 8–9% of all observed core-collapse SNe (Smith et al. 2011; Li et al. 2011), so the physical trigger of the most violent precursors only operates in a subset of core-collapse events.

* Email: nathans@as.arizona.edu

A key issue is the timing of this mass loss. Are these erup-

tions synchronized to go off just before the SN owing to instabilities in the final Ne, O, and Si burning stages of their progenitors (Quataert & Shiode 2012; Shiode & Quataert 2014; Smith & Arnett 2014)? We suspect that pre-SN instability may be more widespread than indicated by the observed fraction of traditional SNe IIn noted above, since these may be only the most extreme manifestation of a more generic phenomenon (Smith & Arnett 2014). At a less extreme level, some SNe show Type IIn signatures for just a day or so after explosion (Gal-Yam et al. 2014; Smith et al. 2015; Khasov et al. 2016; ?; Quimby et al. 2007; Shivvers et al. 2015), which can only be seen if they are discovered early. At the other extreme, major mass-loss episodes also seem to precede core collapse by centuries or millennia. In the latter case, it could take months or years for the blast wave to reach the CSM. This may often go undetected as follow-up SN observations rarely extend past the first few months because of sensitivity limits or observers' compulsion to turn their attention to newer SNe.

There are some observed cases of significantly delayed onset of CSM interaction. Most famously, SN 1987A began to collide with its CSM ring nebula after roughly a decade (Sonnenborn et al. 1998; Michael et al. 1998), and in this case velocities of the ring nebula indicate that it was ejected 10–20 thousand years prior (Meaburn et al. 1995; Crotts & Heathcote 2000). This interaction was relatively modest compared to that of SNe IIn, however, and did not lead to a huge increase in luminosity that would have been observable in a distant galaxy. An interesting case is SN 2008iy, which did show a large increase in luminosity after a delay. Initially it had an absolute magnitude of about -16.5 , similar to a normal SN II-P with no CSM interaction, but then brightened to about -19 mag after 400 days as the SN caught up to a massive shell ejected a century earlier (Miller et al. 2010a). SN 2001em and more recently SN 2014C represent cases in which a stripped-envelope explosion crashed into a H-rich shell after a year or more and developed strong, relatively narrow H α emission (Chugai & Chevalier 2006; Milisavljevic et al. 2015; Margutti et al. 2016). Infrared (IR) echoes from CSM dust illuminated by the SN itself (Wright 1980) or by ongoing interaction (see, e.g., Fox et al. 2011) also provide evidence for massive distant shells. An extreme case is SN 2006gy, which — in addition to its $\sim 20 M_{\odot}$ shell ejected only 8 yr before core collapse (Smith et al. 2010) — also had another more distant shell of $10\text{--}20 M_{\odot}$ ejected $\sim 10^3$ yr earlier (Smith et al. 2008b; Miller et al. 2010b; Fox et al. 2015). Yet another case of a very massive dust shell seen as an echo is SN 2002hh (Barlow et al. 2005), although interestingly, this aging SN does not yet show signs of shock interaction with this shell even though it probably should have reached it by now (Andrews et al. 2015). For SN 2005ip, the SN considered in this paper, Fox et al. (2013) interpreted the IR echo properties as indicating a past major mass-loss outburst that was followed by a less intense wind.

We therefore have mounting evidence of major mass-loss episodes that precede core collapse by centuries or millennia, and not just in the few years beforehand. If the precursor outbursts of SNe IIn in the decade prior to core collapse can be linked to final nuclear burning phases (Quataert & Shiode 2012; Shiode & Quataert 2014; Smith & Arnett 2014), then what can give rise to older mass ejections? Wave-driven mass loss during Ne and O burning can only drive significant mass loss for a few years before core collapse, according to current models (Quataert & Shiode 2012; Shiode & Quataert 2014). Additional observations are needed to constrain the physical parameters and time dependence, but there is mounting evidence of enhanced mass

loss on much longer timescales than Ne and O burning. Woosley (2016) notes that the pulsational pair mechanism can produce mass-loss eruptions that precede core collapse on a variety of timescales, but these come from very massive stars and should be relatively rare (and the eruptions might not be punctuated by an energetic SN, as material falls back to a black hole). This poses an interesting observational question: What fraction of SNe (including otherwise normal SNe) have much more extended dense shells? For this reason, we have been monitoring some old, nearby SNe to look for changes in their late-time interaction.

In this paper we revisit the aging event SN 2005ip, an unusual SN IIn located in the host galaxy NGC 2906 at a distance of ~ 30 Mpc. Smith et al. (2009a) presented the optical photometric and spectroscopic evolution over the first ~ 1000 d, while Fox et al. (2009) discussed the IR photometric evolution over the same time period. SN 2005ip was notable among SNe IIn for its sustained strong CSM interaction at late times, its rather unusual high-ionization spectrum with strong coronal emission lines and a strong blue pseudocontinuum, and its strong IR emission from dust. SN 2005ip showed some evidence for the formation of new dust at these early times (Smith et al. 2009a; Fox et al. 2009), although Fox et al. (2010) concluded that the IR emission was likely produced by a combination of new dust formation and an IR echo from pre-existing CSM dust. Fox et al. (2010) considered distant dust shells of various radii to explain the IR echo, and Fox et al. (2011, 2013) favoured a dust shell located ~ 0.03 pc from the star to explain the IR echo evolution. This is similar to the radius where we infer late-time CSM interaction in SN 2005ip, so it is possible that the variability of H α emission that we report here is caused by the ejecta hitting shells that were seen as an IR echo at earlier times. This is discussed below.

Overall, the early-time data suggested a scenario wherein the SN blast wave was interacting with a very dense and clumpy RSG wind having a mass-loss rate of more than $2 \times 10^{-4} M_{\odot} \text{ yr}^{-1}$ and likely around $10^{-3} M_{\odot} \text{ yr}^{-1}$ (Smith et al. 2009a). This points to an extreme RSG akin to VY CMa, rather than a normal RSG like α Ori (Smith et al. 2009b).

Subsequent papers followed the continuing evolution of SN 2005ip as it faded during the decade after explosion. By 1800–2400 d after discovery, the H α flux had dropped by about a factor of 10 (Stritzinger et al. 2012), although this was still much stronger than typical interacting SNe at a comparable epoch. Stritzinger et al. (2012) also drew similar conclusions as Smith et al. (2009a) concerning the evidence for dust formation and the nature of the progenitor's mass loss, and Stritzinger et al. (2012) mentioned that the X-ray and H α fluxes seem to provide consistent results. Fox et al. (2015) also presented a late-time (day 3024) optical spectrum of SN 2005ip, showing evidence for continued interaction. Katsuda et al. (2014) studied the evolution of X-ray emission from SN 2005ip during the ~ 2400 d after discovery. They found that the X-ray luminosity was roughly constant until 2009 and dropped by a factor of two by 2012. They also showed that the absorbing column density (N_{H}) appeared to be steadily declining during the same time period. This prompted Katsuda et al. (2014) to suggest that the progenitor had ejected a massive CSM shell in the centuries before explosion, and that after ~ 6 yr, the blast wave was finally emerging from this shell, which they estimated to have a total mass of $\sim 15 M_{\odot}$ swept up by that time. This implied that the epoch of CSM interaction was coming to an end in SN 2005ip.

Here we show that CSM interaction clearly has not yet finished. The CSM interaction intensity, traced by H α luminosity, continued to decline very slowly until about mid 2015. After that

Table 1. Late-Time Optical Spectroscopy of SN 2005ip

UT Date (y m d)	Day ^a	Tel./Inst.	Res. $\frac{\lambda}{\Delta\lambda}$	$F(\text{H}\alpha)^b$ $10^{-16} \text{ erg s}^{-1} \text{ cm}^{-2}$
2011 Jan. 13	1895	MMT/BC	4500	476
2012 Jan. 02	2249	MMT/BC	4500	259
2012 Apr. 16	2354	MMT/BC	4500	255
2012 Nov. 24	2576	MMT/BC	4500	220
2014 May 01	3099	Keck/LRIS	1500	156
2015 Mar. 23	3425	MMT/BC	4500	40.8 ^c
2015 Nov. 22	3668	LBT/MODS	1000	33.9
2015 Dec. 16	3692	Keck/DEIMOS	2500	81.3
2016 Feb. 16	3755	MMT/BC	4500	113
2016 Mar. 02	3770	Keck/DEIMOS	2500	105

^aHere and elsewhere, we note “Day” as the day from discovery. For SN 2005ip and SN 1988Z this is an unknown amount after explosion, whereas for SN 1993J and SN 1998S the discovery is likely to have been within a day or so of explosion.

^bAssumed uncertainty is $\pm 25\%$, owing mainly to the systematic uncertainty of the placement of the standard star within the slit aperture (which is, however, difficult to quantify). Measurement uncertainty due to noise in the spectra is much lower.

^cThere were some thin clouds that came in during subsequent exposures (not included in this estimate), so we increased the uncertainty for this observation when plotted in Figure 1.

Table 2. Late-Time Optical Spectroscopy of SN 1988Z

UT Date (y m d)	Day	Tel./Inst.	Res. $\frac{\lambda}{\Delta\lambda}$	$F(\text{H}\alpha)^a$ $10^{-16} \text{ erg s}^{-1} \text{ cm}^{-2}$
1994 Jun. 10	2006	Keck/LRIS	1500	67.8
1995 Nov. 28	2542	Keck/LRIS	1500	56 ^b
2003 Jan. 06	5138	Keck/LRIS	1500	21.5
2007 Feb. 16	6640	Keck/DEIMOS	2500	19.6
2010 Feb. 15	7735	Keck/DEIMOS	2500	12.7
2012 May 17	8557	Keck/LRIS	1500	10.5

^aAssumed uncertainty is $\pm 25\%$, owing mainly to the systematic uncertainty of the placement of the standard star within the slit aperture (which is, however, difficult to quantify). Measurement uncertainty due to noise in the spectra is much lower.

^bWe increase the uncertainty on this point because of possible calibration issues. We normalized to the flux of [S II] emission lines from underlying H II regions in the same aperture at other epochs.

time, however, the H α showed abrupt variations, including a brightening by late 2015 and early 2016. The radio and X-ray emission was also bright in early 2016, as described below. This indicates that the blast wave has continued to run into a distant CSM shell or torus. We explore possible explanations for the origin of this CSM and implications for the pre-SN evolution of massive stars. For comparison, we also discuss similar continued interaction via late-time H α emission seen in newly obtained spectra of SNe 1988Z, 1993J, and 1998S.

2 OBSERVATIONS

2.1 Visual-Wavelength Spectroscopy

We obtained late-time optical spectroscopy of SN 2005ip over several epochs since our previous study (Smith et al. 2009a). These observations included the Bluechannel (BC) spectrograph on the 6.5 m Multiple Mirror Telescope (MMT), the Multi-Object Double Spectrograph (MODS; Byard & O’Brien 2000) on the Large Binocular Telescope (LBT), the Low-Resolution Imag-

Table 3. Late-Time Optical Spectroscopy of SN 1993J

UT Date (y m d)	Day	Tel./Inst.	Res. $\frac{\lambda}{\Delta\lambda}$	$F(\text{H}\alpha)^a$ $10^{-16} \text{ erg s}^{-1} \text{ cm}^{-2}$
2004 Nov. 14	4249	Keck/LRIS	1500	73
2010 Feb. 06	6159	Keck/LRIS	1500	47
2010 Feb. 15	6168	Keck/DEIMOS	2500	13
2012 Apr. 29	6972	Keck/LRIS	1500	35
2012 May 17	6990	Keck/LRIS	1500	43
2013 Feb. 17	7266	Keck/DEIMOS	2500	400
2015 Feb. 20	7999	Keck/LRIS	1500	14
2016 Feb. 10	8353	Keck/LRIS	1500	82

^aAssumed uncertainty is $\pm 30\%$, owing mainly to the systematic uncertainty of the placement of the standard star within the slit aperture (which is, however, difficult to quantify), plus some uncertainty produced by blending with an adjacent oxygen line. Measurement uncertainty due to noise in the spectra is lower.

Table 4. SN 2005ip on 2016 Feb. 4; VLA

Frequency (GHz)	Flux Density (mJy)	Uncertainty (mJy)
5.0	1.18	0.04
7.4	0.92	0.04
8.5	0.86	0.03
11.0	0.77	0.03

ing Spectrometer (LRIS; Oke et al. 1995) mounted on the 10 m Keck I telescope, and the Deep Imaging Multi-Object Spectrograph (DEIMOS; Faber et al. 2003) on Keck II. Details of the spectral observations including measurements of the total H α line flux are summarized in Table 1, and the spectra are shown in Figure 1. Standard reductions were carried out using IRAF¹ including bias subtraction, flat-fielding, and optimal spectral extraction (see, e.g., Kelson 2003). Flux calibration was achieved using spectrophotometric standards observed at similar airmass to that of each science frame, and the resulting spectra were median combined into a single one-dimensional spectrum. For one observation noted in Table 1, the flux calibration was suspect owing to clouds that came in during subsequent exposures. For this date (day 3425) we increase the uncertainty in Figure 6 to $\pm 50\%$.

SN 1988Z: In our study, we find it useful to compare the evolution of SN 2005ip to that of a few other well-studied, geriatric SNe with late-time interaction. SN 1988Z is a prototypical, long-lasting, and radio-luminous SN IIn that has been studied in detail by several authors (Filippenko 1991; Stathakis & Sadler 1991; Turatto et al. 1993; Van Dyk et al. 1993; Chugai & Danziger 1994; Fabian & Terlevich 1996; Aretxaga et al. 1999; Williams et al. 2002; Schlegel & Petre 2006). In particular, Aretxaga et al. (1999) have compiled multiwavelength data, including H α fluxes, up to day ~ 3000 . We have obtained additional unpublished late-time spectra of this aging SN IIn using the Keck Observatory, with both LRIS and DEIMOS. These observations, including estimated H α line fluxes, are summarized in Table 2 and almost triple the time baseline for this object. This series of new late-time spectra of SN 1988Z is shown in Figure 2. These spectra have been corrected

¹ IRAF, the Image Reduction and Analysis Facility, is distributed by the National Optical Astronomy Observatory, which is operated by the Association of Universities for Research in Astronomy (AURA), Inc., under cooperative agreement with the National Science Foundation (NSF).

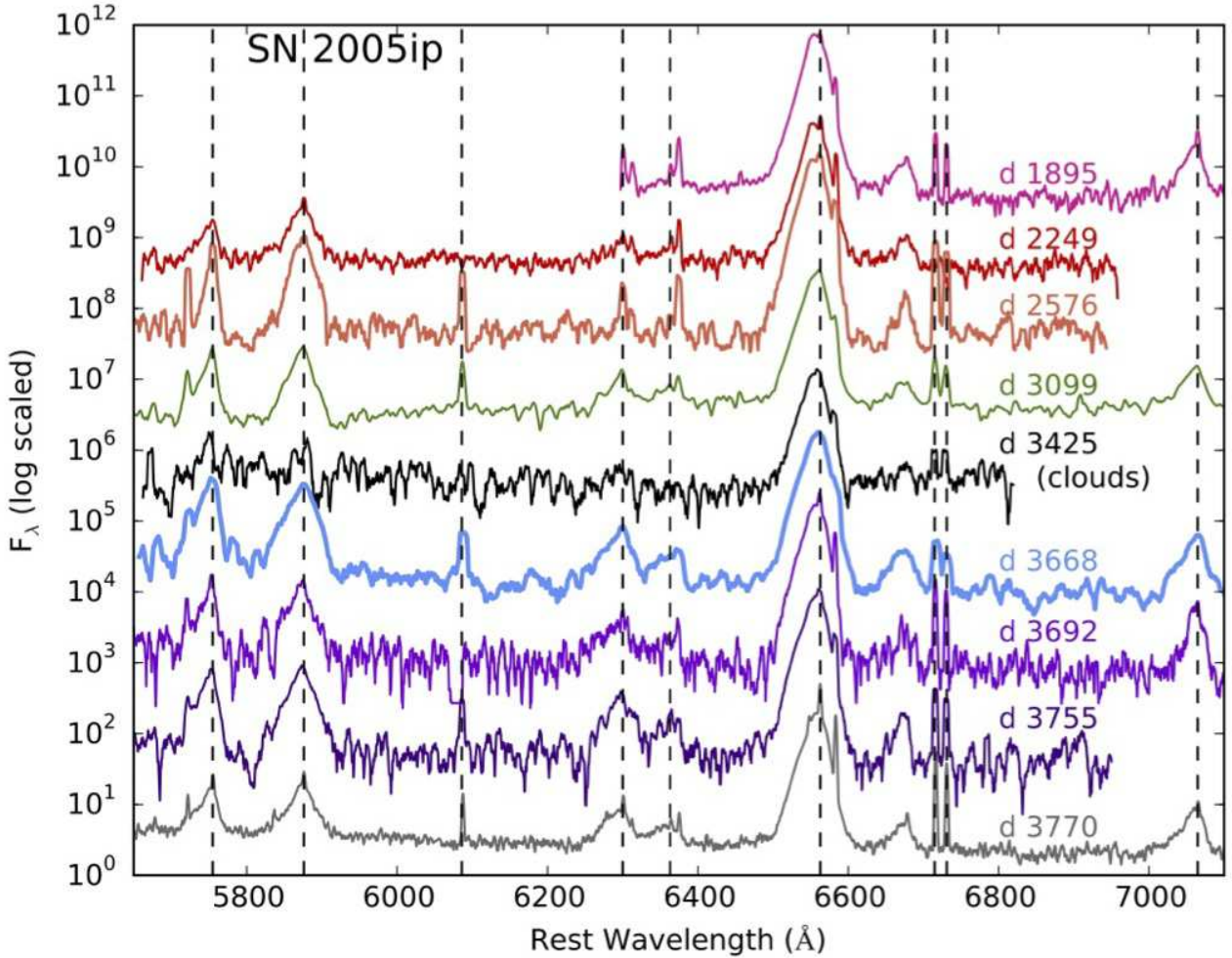


Figure 1. Late-time spectra of SN 2005ip (see Table 1) normalized to the red continuum level. The spectra plotted in thin red-orange-green colours represent the appearance of the spectrum in its late-time decline. The black and light-blue spectra are when the $H\alpha$ flux reached its minimum in 2015, while the purple/blue/grey colours document the resurgence of CSM interaction. See Figure 2 for line identifications.

for a redshift of $z = 0.022$, but no reddening correction has been applied as in previous studies (Aretxaga et al. 1999). When we plot the $H\alpha$ line luminosity in Figure 6, we first subtract a constant flux of $7 \times 10^{-16} \text{ erg s}^{-1} \text{ cm}^{-2}$, which is the mean value of the narrow $H\alpha + [N \text{ II}]$ line fluxes in late-time spectra (this is only significant for the last epochs). We attribute this constant narrow emission to contamination by coincident or nearby H II region emission, or perhaps unshocked distant CSM. Since we compare the $H\alpha$ luminosity of SN 2005ip to SN 1988Z and also to other well-studied late interactors, we obtained late-time spectra to extend the temporal coverage of two additional prototypical SNe.

SN 1993J: We procured several late-time spectra of SN 1993J, most recently on 2016 Feb. 10 using LRIS on Keck I. SN 1993J was a Type Ib event rather than a Type IIc, but it was very nearby in M81, was discovered within about 1 day of explosion, and has shown strong, long-lived CSM interaction that has given rise to a high radio luminosity and prominent optical/UV emission lines for more than a decade after explosion (Fransson et al. 1996;

Matheson et al. 2000; Bietenholz et al. 2002). Table 3 summarizes our late-time spectra reported here, including a measurement of the total $H\alpha$ line flux in the calibrated spectra. Here the uncertainty is dominated by the fact that the blue side of $H\alpha$ is blended with a strong oxygen line, as well as uncertainty from possible slit losses. Qualitatively, the spectral appearance of SN 1993J changes very little at these late epochs after day 4000, and even resembles the day 2454 spectrum presented by Matheson et al. (2000). The most recent epoch is illustrated in the bottom panel of Figure 2 in dark green; we also show two earlier epochs on days 4249 and 6159 in a lighter shade of green for comparison. Although some of the emission lines have weakened with time, the line profiles and overall appearance of the spectrum have not changed much.

SN 1998S: This has long been considered a prototypical SN IIc, which was discovered within about a day of explosion, but its early CSM interaction was on the weak side compared to most SNe IIc (Leonard et al. 2000; Fassia et al. 2001). SN 1998S did, however, exhibit strong continued CSM interaction at late times

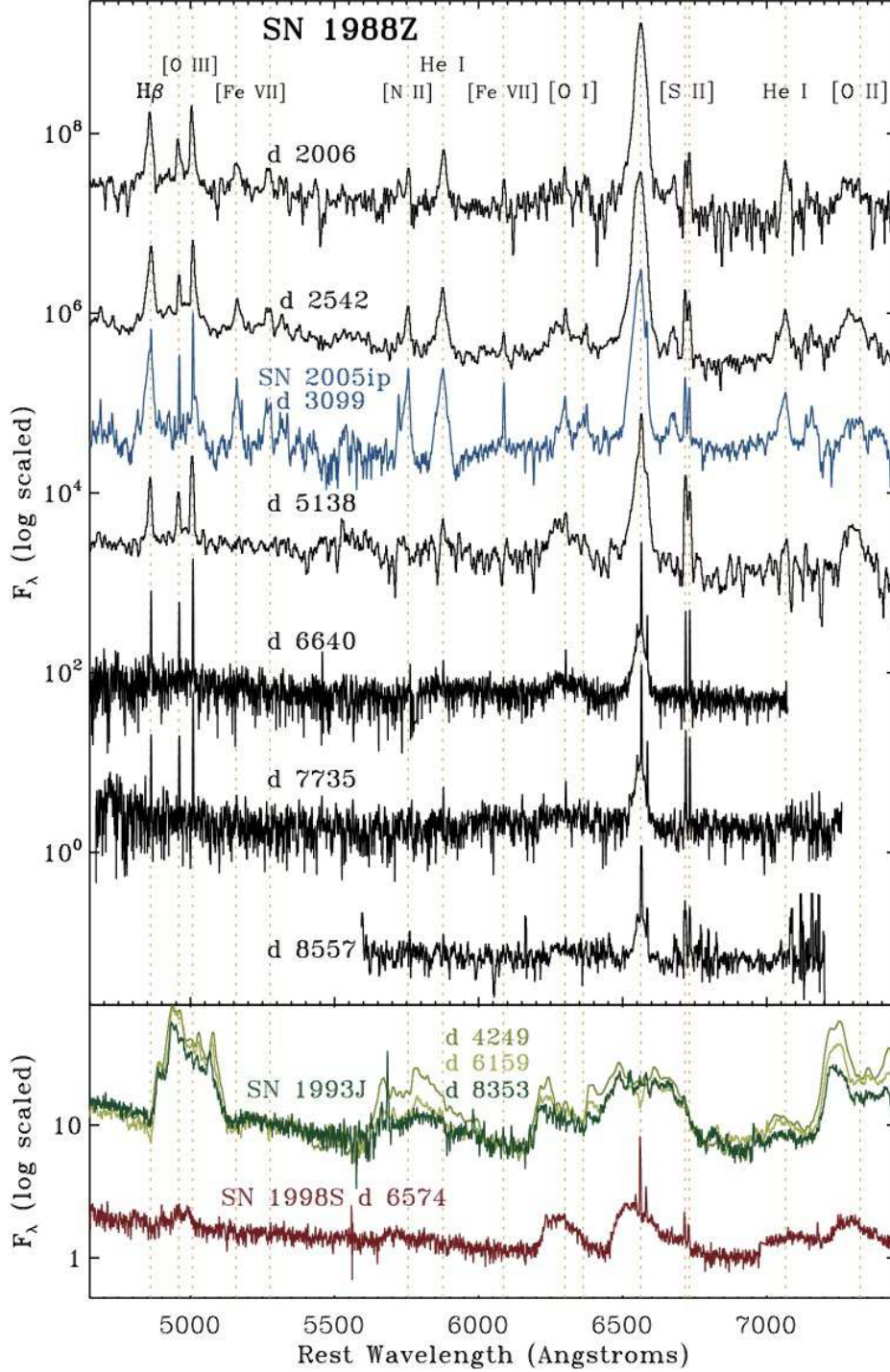


Figure 2. The top panel shows late-time spectra of SN 1988Z (see Table 2). Vertical dashed orange lines identify specific emission lines. We include the day 3099 spectrum of SN 2005ip (blue) for comparison. The bottom panel shows some of our additional late-time spectra of SN 1993J and SN 1998S.

(Pozzo et al. 2004; Mauerhan & Smith 2012). We obtained a late epoch of SN 1998S on 2016 Mar. 1 using DEIMOS on Keck II, extending the spectral evolution by ~ 1500 d compared to published data. The last previously published spectrum of SN 1998S (Mauerhan & Smith 2012) was obtained on day 5079, and our new spectrum corresponds to day 6574. Qualitatively, the appearance of this spectrum shows little change compared to the last one published by Mauerhan & Smith (2012). For this spectrum,

however, we measure a strong H α line flux of $(2.15 \pm 1) \times 10^{-15}$ erg s $^{-1}$ cm $^{-2}$, which is several times higher than our previous flux measurement (Mauerhan & Smith 2012). The uncertainty is likely to be dominated by absolute flux calibration and slit placement as noted above for SN 2005ip and SN 1988Z, but this increase appears to be significant. The new spectrum of SN 1998S is shown in the bottom panel of Figure 2.

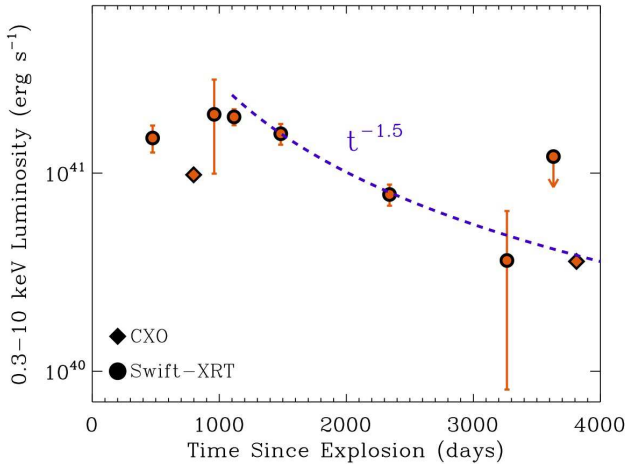


Figure 3. X-ray luminosity evolution of SN 2005ip in the 0.3–10 keV energy band. Circles refer to *Swift* data, and the diamonds are fluxes from *Chandra* data reported by (Katsuda et al. 2014) as well as from our new *Chandra* observations (see text).

2.2 Radio

We observed the position of SN 2005ip with the Karl G. Jansky Very Large Array (VLA; Program 16A-101, PI Kilpatrick) starting on 2016 Feb. 4 (day 3743 after discovery) at 09:47:29 (UT dates are used throughout this paper), at mean frequencies of 6.2 GHz and 9.8 GHz (with side-bands centred at 5.0, 7.4, 8.5, and 11.0 GHz). We obtained 14 min of on-source time for each frequency, and used 3C286 and J0925+0019 for bandpass/flux and gain calibration, respectively. Following standard procedures in the Astronomical Image Processing System (AIPS; Greisen 2003) for data calibration and analysis, we detect a bright source located at $\alpha = 09^{\text{h}}32^{\text{m}}06.41^{\text{s}}$, $\delta = +08^{\circ}26'44.36''$ (J2000; $\delta\alpha = 0.05''$, $\delta\delta = 0.03''$), consistent with the optical position. We measure flux densities and 1σ uncertainties for the upper and lower side-bands using AIPS/JMFIT. The radio detections are listed in Table 4. The radio spectral index of SN 2005ip is $\alpha = 0.55 \pm 0.11$, which is consistent with optically thin emission observed from SNe II (Weiler et al. 2002). We postpone a more detailed analysis of the radio data to a later paper that will examine its temporal variability.

2.3 Swift-XRT

The X-Ray Telescope (XRT; Burrows et al. 2005) onboard the *Swift* satellite (Gehrels et al. 2004) started observing SN 2005ip on 2007 Feb. 14 (475 days since discovery). Late-time observations of SN 2005ip have been carried out until 3630.5 days, as part of a *Swift* fill-in program (PI Margutti).

XRT data have been analyzed using HEASOFT (v6.18) and corresponding calibration files, following standard procedures (see Margutti et al. 2013 for details). In particular, our rebinning scheme requires a minimum of 20 photons in the source region and an inferred source count rate at least 3σ above the background level to yield a detection. Compared to the previous compilation by Katsuda et al. (2014), our campaign extends the X-ray monitoring of SN 2005ip from ~ 2400 days to ~ 3600 days since explosion, and reveals a continuation of the fading X-ray emission with time. The resulting luminosity light curve is shown in Fig. 3.

For the flux calibration of *Swift*-XRT data acquired at $t < 2400$ days we employ the spectral parameters of the one-

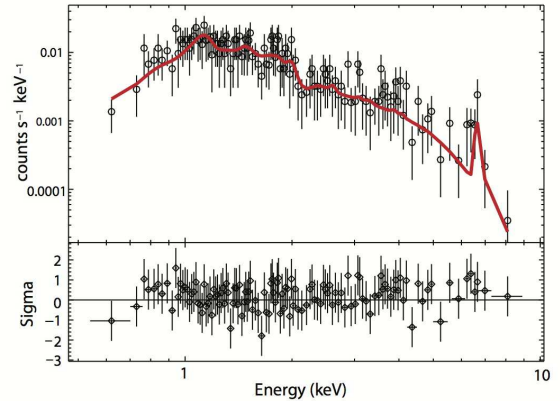


Figure 4. *Chandra* ACIS-S energy spectrum of SN 2005ip from 2016 Apr. 3. The red curve is a thermal plasma model (see text), with model residuals shown in the lower panel.

component model derived by Katsuda et al. (2014) (their Table 2) with a shock temperature evolution $T \propto t^{-0.2}$. For *Swift*-XRT data acquired at $t > 3000$ days we adopt the spectral parameters constrained by our latest *Chandra* spectrum (see below). Figure 3 shows the X-ray evolution of SN 2005ip in the 0.3–10 keV energy range as captured by the *Swift*-XRT and *Chandra* in the first ~ 4000 days since explosion. The steep decline ($L_x \propto t^{-1.5}$) at late times suggests that the shock is sampling a steeply decaying environment density profile $\rho \propto r^{-s}$ with $s > 2$ (Fransson & Björnsson 1998).

2.4 Chandra ACIS

SN 2005ip was observed with the *Chandra* X-ray Observatory (CXO) and Advanced CCD Imaging Spectrometer (ACIS) on 2016 Apr. 3 (3812 days) under a single-epoch DDT program (PI Mauershan, ID 18802). The ACIS-S array was used and the total on-source exposure time was 35.59 ks.

Photometry and energy spectra were extracted using the `specextract` package within the HEASOFT *Ciao* software suite. The point source associated with SN 2005ip yielded 820 counts within a circular aperture $2''$ in radius. A $5''$ radius background annulus surrounding the source aperture yielded 121 counts. The energy spectrum of the source is shown in Figure 4. Note the apparent detection of Fe $K\alpha$ emission near 6.8 keV.

The source and background spectra were modeled simultaneously using the *Sherpa* package. An absorbed single-temperature thermal plasma model (*apec*) having solar abundances as defined by Asplund et al. (2009) was fit to the source for photon energies in the range 0.5–8.0 keV, and a simple power law was used to fit to the background. The He, C, N, O, and Fe elemental fractions, by number relative to H, are 8.51×10^{-2} , 2.69×10^{-4} , 6.76×10^{-5} , 4.90×10^{-4} , and 3.16×10^{-5} , respectively. A C -statistic was used in the fitting. We fixed an equivalent interstellar neutral hydrogen column density of $N_{\text{H}}(\text{ISM}) = 3.7 \times 10^{20} \text{ cm}^{-2}$, adopting this value from Katsuda et al. (2014), and allowed for an additional intrinsic source of absorption for the SN. Our best fit yielded $N_{\text{H}}(\text{SN}) = 1.9^{+0.8}_{-0.7} \times 10^{21} \text{ cm}^{-2}$ and a plasma temperature of $kT = 5.0^{+1.1}_{-0.9} \text{ keV}$. The associated uncertainties are 90% confidence envelopes ($\sim 1.6\sigma$). The absorbed energy flux is

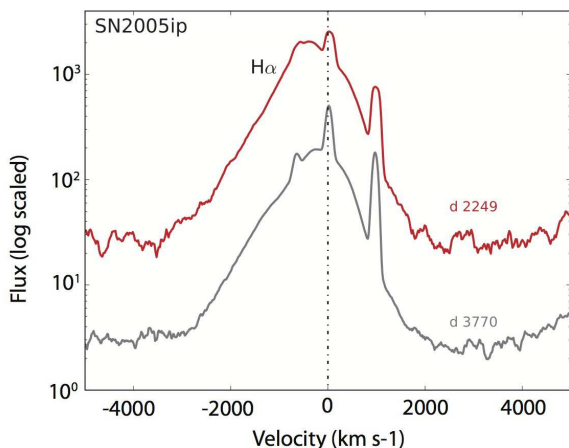


Figure 5. A detail of the observed $H\alpha$ line profile, with velocity relative to the centroid of the narrow component. This shows two of the higher-resolution spectra obtained with MMT/Bluechannel (day 2249) and Keck/DEIMOS (day 3770), before and after the dip in 2015, respectively.

$F_{\text{abs}} = 2.36^{+0.06}_{-0.02} \times 10^{-13} \text{ erg s}^{-1} \text{ cm}^{-2}$ (0.5–8.0 keV) and the unabsorbed model flux is $F_{\text{unabs}} = 2.86^{+0.12}_{-0.08} \times 10^{-13} \text{ erg s}^{-1} \text{ cm}^{-2}$. For our adopted distance the flux implies an X-ray luminosity of $L_X = 3.2 \times 10^{40} \text{ erg s}^{-1}$ for the SN at epoch 3812 days. We also experimented with fitting the data using a χ^2 statistic with a Gehrels variance function, and obtained a reduced χ^2 value of 43.6 for 65 degrees of freedom. The resulting physical parameters are consistent with those from the C statistic, quoted above. The model fit is also shown in Figure 4.

3 RESULTS

3.1 $H\alpha$ Evolution of SN 2005ip

Figure 1 shows our newly obtained series of late-time optical spectra of SN 2005ip, and Figure 5 displays the $H\alpha$ line profile in a few epochs with the best signal-to-noise ratio. In addition to $H\alpha$, the spectrum shows consistent emission from other lines commonly seen in late-time spectra of strongly interacting SNe IIn. Here we focus mainly on the $H\alpha$ line, since it is the dominant line in the spectrum of SNe IIn observed at late times, and is a good proxy for the strength of interaction.

Our higher-resolution spectra (i.e., all but the 2014 May and 2015 Nov. spectra) are able to cleanly resolve the intermediate-width emission of the post-shock gas from the narrow pre-shock CSM or underlying H II region emission (Fig. 5). In these spectra, the intermediate-width component of $H\alpha$ (within about $\pm 2000 \text{ km s}^{-1}$) has a consistent profile shape, which is asymmetric and shifted to the blue. The peak of this emission is located roughly at -200 to -400 km s^{-1} , shifting toward more positive velocities with time. This asymmetric blueshifted profile was seen at early times in the broad and intermediate-width lines (Smith et al. 2009a), and was attributed to new dust formation in the SN ejecta or in the post-shock gas. Blueshifted lines with this type of shape can arise simply from occultation of the far side by the SN photosphere at early times (Smith et al. 2012; Fransson et al. 2014; Dessart et al. 2015), but the fact that the blueshifted asymmetry persists for a decade in SN 2005ip, long after the continuum opacity of the photosphere has vanished, means that the blocking of the red side of the lines must be caused by dust mixed within the SN

(or to intrinsically asymmetric CSM). Much of the dust is likely to be mixed in the post-shock region where the intermediate-width $H\alpha$ originates, since even early-time spectra showed a blueshift in lines formed within the post-shock shell, as well as in the broad SN ejecta lines (Smith et al. 2009a). The narrowest components from the pre-shock CSM are unresolved or only marginally resolved in our spectra, indicating expansion speeds of 80 km s^{-1} or less (Fig. 5).

The temporal evolution of the $H\alpha$ line luminosity is shown in Figure 6. This plot uses $H\alpha$ line fluxes in the first 1000 d from our earlier paper (Smith et al. 2009a), and supplements these with our new spectra of SN 2005ip reported here. The line fluxes were converted to $H\alpha$ luminosity with the same assumptions as in our earlier study. The $H\alpha$ luminosity remains roughly constant for the first 1000 d, as we noted earlier, and then declines slowly over the next several years as found previously by Stritzinger et al. (2012). Our new spectra show that this slow decline continued to around day ~ 3600 (mid 2015), when the $H\alpha$ luminosity was in decline, and then suddenly reversed to be on a quick rise that has continued to the time of writing. Additional monitoring will be needed to determine how high it will rise, if it levels off, or fades again. Possible causes of this are discussed further in Section 4.

Figure 6 also compares the $H\alpha$ luminosity of SN 2005ip to that of several other SNe with strong late-time interaction. We see here that SN 2005ip really is quite unusual, with a sustained $H\alpha$ luminosity that was essentially the same as the current record holder for such interaction: SN 1988Z (see below). At days 1000–2000, the $H\alpha$ luminosity was 2 orders of magnitude stronger than in some other well-studied objects like SN 1998S (Mauerhan & Smith 2012), SN 1980K (Milisavljevic et al. 2012), and SN 1993J (Chandra et al. 2009), and an order of magnitude stronger than in the SN IIn PTF11iqb (Smith et al. 2015). The late-time CSM interaction in these other objects can be explained by a very strong RSG wind with $10^{-4} M_{\odot} \text{ yr}^{-1}$ (Mauerhan & Smith 2012), but SN 2005ip and SN 1988Z are clearly more extreme situations. Thus, the $H\alpha$ luminosity implies that around 4000 days after explosion, the shock is interacting with a wind that had a mass-loss rate of at least $10^{-3} M_{\odot} \text{ yr}^{-1}$. With a CSM speed² around 40 km s^{-1} , this implies that the high mass-loss rate was occurring within a few thousand years before core collapse. This, in turn, requires several M_{\odot} being lost from the star in the last few millennia of its life. Our estimate is conservative compared with some others, which favour higher rates of $\gtrsim 0.01 M_{\odot} \text{ yr}^{-1}$ and total CSM masses greater than $10 M_{\odot}$ (Katsuda et al. 2014; Stritzinger et al. 2012).

In our earlier paper (Smith et al. 2009a), we drew comparisons between SN 2005ip and SN 1988Z, including a direct comparison of the $H\alpha$ luminosity. During the first several hundred days, SN 2005ip was significantly less luminous in both $H\alpha$ and continuum emission. However, during this time SN 2005ip remained roughly constant in $H\alpha$ luminosity, while SN 1988Z steadily declined. Figure 6 extends this same comparison, and shows that by day 1000 the two objects had about the same luminosity, and for the rest of its first decade, SN 2005ip was an almost exact twin of SN 1988Z in terms of its CSM interaction strength traced by $H\alpha$. As in our previous paper, Figure 6 incorporates $H\alpha$ luminosities for SN 1988Z published by Turatto et al. (1993), extended to almost

² This is a guess, but is lower than the 80 km s^{-1} resolution limit of our data, and similar to CSM speeds for SN 1998S seen in echelle spectra (Shivvers et al. 2015).

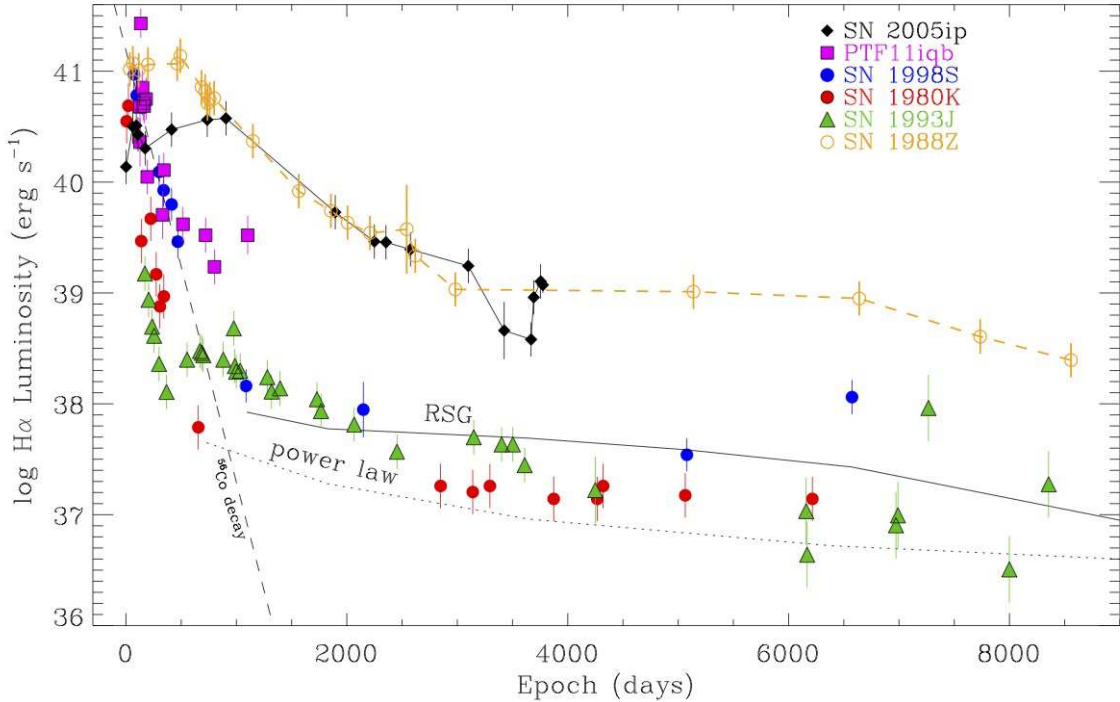


Figure 6. Evolution of the total H α luminosity for SN 2005ip (black diamonds) compared to observations of other representative SNe with ongoing CSM interaction, as well as expected trends for a RSG wind profile (Chevalier & Fransson 1994) and radioactive decay (dashed line). This figure is adapted from Smith et al. (2015), which was adapted from Mauerhan & Smith (2012). H α luminosities for SN 1998S are from Mauerhan & Smith (2012), SN 1980K from Milisavljevic et al. (2012), SN 1993J from Chandra et al. (2009), and PTF11iqb from Smith et al. (2015). For SN 1988Z, we use H α fluxes from Turatto et al. (1993) as described in our previous paper (Smith et al. 2009a), extended to almost day 3000 by Aretxaga et al. (1999), plus our own measurements from unpublished spectra taken at later times of SN 1988Z (see Table 2), SN 1993J, and SN 1998S. The dashed black line shows the expected rate of fading for radioactive decay luminosity from ^{56}Co , for comparison.

day 3000 by Aretxaga et al. (1999). We also supplement these published H α luminosities with measurements from our own spectra of SN 1988Z (see Table 2).

With its recent resurgence in H α luminosity, SN 2005ip equals SN 1988Z again at a comparable epoch, making it tied as the record holder for the highest late-time H α luminosity at +10 yr. Integrating through time in Figure 6, the total energy radiated by SN 2005ip in the H α line alone is 4×10^{48} erg. For comparison, the total integrated 0.3–10 keV X-ray energy is about a factor of 10 larger at $\sim 4 \times 10^{49}$ erg, and the integrated optical luminosity yields a similar total radiated energy of $\sim 4 \times 10^{49}$ erg. This is certainly an underestimate of the total radiated energy, since we applied no correction for flux at other wavelengths. The asymmetric blueshifted profiles of H α , in particular, suggest some dust extinction in SN 2005ip (with a lack of such evidence for dust extinction in SN 1988Z); correcting for this could raise the H α and continuum luminosities further, and thus make SN 2005ip significantly more luminous than SN 1988Z. The radiated energy so far is therefore likely to be at least 10^{50} erg for SN 2005ip. The kinetic energy imparted to the swept-up CSM shell (about $10 M_{\odot}$ accelerated to $\sim 2000 \text{ km s}^{-1}$) is roughly 4×10^{50} erg. Thus, CSM interaction may have already tapped a substantial fraction of the explosion energy in SN 2005ip; remaining kinetic energy of the freely expanding ejecta that are still inside the reverse shock may power SN 2005ip for the next decade. It will be interesting to see where it goes from here. A significant detail is that after it rebrilliantened, the spectrum showed stronger emission from the intermediate-width components of [O I] $\lambda\lambda 6300, 6364$, which had only shown narrow

pre-shock CSM emission before that time. This may hint that we are starting to see an increased contribution from the reverse-shock luminosity (see Section 3.3 below).

3.2 Very Late-time Evolution of SN 1988Z

Despite its redshift of 0.022, SN 1988Z has remained detectable for nearly three decades. It was a very luminous radio SN that has been studied extensively as it faded slowly after discovery, showing remarkable longevity in the radio, X-rays, and optical emission lines like H α (Filippenko 1991; Stathakis & Sadler 1991; Turatto et al. 1993; Van Dyk et al. 1993; Chugai & Danziger 1994; Fabian & Terlevich 1996; Aretxaga et al. 1999; Williams et al. 2002; Schlegel & Petre 2006). It has been compared to SN 1986J, and most studies of its first decade and a half favour the interpretation that it is powered by an energetic explosion (as much as $\sim 10^{52}$ erg; Aretxaga et al. 1999) from a massive progenitor (an initial mass of something like 20–30 M_{\odot} or more), that was interacting with roughly $10 M_{\odot}$ produced by a star that had a wind with a mass-loss rate of $\sim 10^{-3} M_{\odot} \text{ yr}^{-1}$ for $\sim 10^4$ yr before core collapse. The rate of decline in H α and radio suggested that the mass-loss rate ramped up in the final millennium before core collapse (Van Dyk et al. 1993; Aretxaga et al. 1999; Williams et al. 2002). Even the somewhat lower mass-loss rate traced by later CSM interaction was extreme, however, allowing SN 1988Z to remain as one of the most radio luminous SNe even after a decade, matched only by SN 2005ip.

Here we present a series of optical spectra, listed in Table 2

and shown in Figure 2, which extend this late-time evolution from the mid-1990s to the present epoch. We find that SN 1988Z’s strong CSM interaction has continued to fade very slowly, indicating a remarkably extended and dense wind into which the blast wave continues to crash. This traces mass loss over $\sim 10^4$ yr preceding core collapse. Based on the luminosity of $H\alpha$ and the character of the optical spectra, we group SN 1988Z’s late evolution into a few different epochs:

(1) *The first 500–3000 days.* This is the phase that has already been studied extensively as noted above. During this time, SN 1988Z showed a steady and very slow decline in radio and $H\alpha$ luminosity, although remaining far more luminous than most SNe having signs of CSM interaction. Williams et al. (2002) noted a possible break in the decline rate of the $H\alpha$ luminosity around day 1000, although this break is not clear in Figure 6 where the decline looks rather continuous within the uncertainties. Of interest in the present paper is that throughout the time period of roughly 1000–3000 days, SN 2005ip was a nearly identical twin of SN 1988Z in terms of its decline rate, its luminosity in the radio (admittedly only a single epoch so far for SN 2005ip), $H\alpha$, and X-rays, and in the appearance of its spectrum. In our previous paper (Smith et al. 2009a) we noted similarities in the spectra of SN 2005ip and SN 1988Z at early times, although SN 2005ip exhibited stronger coronal lines. From day 1000 to 3000, however, their spectra are almost indistinguishable. Figure 2 includes a recent spectrum of SN 2005ip on day 3098 for comparison, which appears very similar to the days 2006 and 2542 spectra of SN 1988Z in the same plot. This phase is characterized by very strong intermediate-width $H\alpha$, a steep $H\alpha/H\beta$ decrement of > 10 , several intermediate-width and narrow coronal lines such as [Fe VII], and intermediate-width lines that indicate very high electron densities in the post-shock gas, such as [N II] $\lambda 5755$ (which is, however, blended with an [Fe VII] line).

(2) *A “plateau” over days 3000–7000.* During this time period, the $H\alpha$ luminosity appears to level-off for a decade. While $H\alpha$ remains constant, the rest of the spectrum shows some interesting changes. The coronal lines and other indicators of high density fade away, leaving mostly narrow H II region lines and broad, weak oxygen lines (possibly from the reverse shock; see below) that are also seen in young SN remnants. The intermediate-width $H\beta$ line also fades, yielding an $H\alpha/H\beta$ ratio that is higher than before (> 30).

(3) *After day 7000.* Eventually, other lines fade away too, leaving only intermediate-width $H\alpha$, which also resumed a decline in flux at these very late times. Even the broad/intermediate-width oxygen lines mostly disappear. Note that in Figure 2, we have subtracted a constant value for the contribution of narrow $H\alpha$ + [N II] emission from underlying H II regions in the spectrum, which typically contributes about 7×10^{-16} erg s $^{-1}$ cm $^{-2}$ in our Keck slit aperture after subtraction of adjacent background. This suggests that SN 1988Z resides in or near a complex of H II regions, providing another possible indication of a high initial mass for the progenitor. At SN 1988Z’s distance of ~ 100 Mpc, however, 1” corresponds to almost 500 pc, which could include a large complex of H II regions like the Tarantula nebula, and is not a very reliable or precise indicator of initial mass. It is, however, a good indicator of a relatively strong ambient UV radiation field.

This last point is interesting in the context of something we discuss later. Namely, Mackey et al. (2014) have suggested that external ionization of an otherwise normal RSG wind can produce a stalled dense shell, which might offer an alternative to very strong

or eruptive mass loss as an origin for SNe IIn.³ Despite its probable location in an H II region, this idea does not seem to apply well to SN 1988Z, which from its earliest phases shows an uninterrupted decline in CSM interaction strength, consistent with a strong shock moving through a freely expanding wind. The total mass of 15–20 M_{\odot} or more of CSM that has been swept up so far by SN 1988Z rules out a normal RSG wind that has been confined to a thin shell, because such shells only contain a fraction (about a third) of the total RSG mass loss, and are therefore expected to have much lower total mass (Mackey et al. 2014). With such a strong wind, the expected location of a stalled shell would probably be different from the models presented by Mackey et al. (2014), however. We return to this issue later, because despite its similarity to SN 1988Z, SN 2005ip does show a rapid interruption of the smooth decline in its CSM interaction strength, which might be indicative of external influence of this sort. This may hint that two otherwise very similar events may have their CSM modified in different ways. Then again, the relatively coarse sampling of SN 1988Z in its past decade does not rule out the possibility of some brief drops or spikes in luminosity indicative of density fluctuations in its CSM. Indeed, one may speculate that the late plateau phase in SN 1988Z’s $H\alpha$ luminosity might represent the shock traversing a relatively constant density, ionized portion of the wind outside such a neutral dense shell. For this reason as well, it will be interesting to see how SN 2005ip behaves in the coming decade as compared to SN 1988Z.

3.3 Line Profiles of Elderly Interactors

All the SNe discussed in this paper show signs of long-lived, strong CSM interaction, but there are interesting differences. Examining Figures 1 and 2, it is clear that both SN 2005ip and SN 1988Z have late-time spectra dominated by their intermediate-width components of $H\alpha$ and other lines, with line widths of about 2000 km s $^{-1}$. Both SN 1993J and SN 1998S have significantly broader line profiles of 5000–10,000 km s $^{-1}$. This difference is probably closely linked to their total $H\alpha$ luminosity. Both SN 2005ip and SN 1988Z are ~ 2 orders of magnitude more luminous than the other two at a comparable late epoch. The combination of higher $H\alpha$ luminosity (as well as higher radio and X-ray luminosities), high-density tracers, and narrower lines likely stems from the same cause: *denser CSM and a radiative forward shock*. If a blast wave is expanding into extremely dense and extended CSM, the forward shock can remain radiative, giving higher CSM interaction luminosity and causing the intermediate-width components to continue to dominate the spectrum as the blast wave continues to expand into the CSM and to decelerate slowly. (Strong global asymmetry or a high degree of clumping can provide very high CSM densities without necessarily having a huge total CSM mass, so an intermediate-width component might also be present at lower luminosity in some cases.)

At lower average CSM densities and luminosities, as in SN 1993J and SN 1998S, radiation from the reverse shock dominates the late-time emission, and so the spectrum exhibits much broader lines from oxygen-rich SN ejecta crossing the reverse

³ Note that this scenario cannot explain the CSM interaction observed at early times in normal SNe IIn, because their narrow emission line components have resolved widths and P-Cygni absorption indicating that the CSM near the star is *outflowing* — i.e., the CSM shells are not stalled and are not ambient material (see Smith 2014). Stalled shells of this sort, however, could potentially influence the shock interaction observed at very late times.

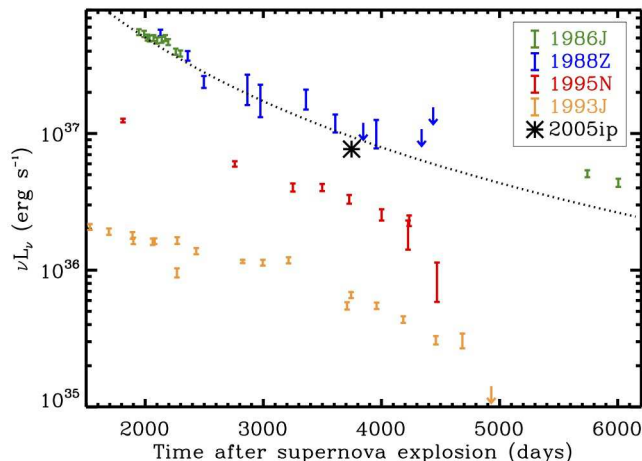


Figure 7. Late-time (1500–6000 days) 5 GHz luminosity observed toward SNe 1986J, 1988Z, 1995N, and 2005ip ($d = 10, 100, 24, 33$ Mpc, respectively; Williams et al. 2002; Bietenholz et al. 2002; Chandra et al. 2009; Smith et al. 2009a). We have assumed that the radio emission from each event is emitted isotropically. The dotted curve shows the best-fit model to late-time (> 1500 day) emission from SN 1988Z.

shock. In our late spectra of SN 1993J, the flat-topped and double-peaked profiles described by Matheson et al. (2000) still persist. These may be the result of interaction with a disk-like CSM, which pinches the waist of the CSM interaction region and makes the reverse shock brighter at the equator. One may envision a reverse-shock geometry similar to that of SN 1987A (France et al. 2015).

Interestingly, we may see a transitional phase in SN 1988Z, where weak and broad oxygen lines remain after the intermediate-width coronal lines have faded (days 5138 and 6640 in Figure 2). In general, though, the lack of strong oxygen lines in most SNe II in at a few hundred days after explosion is most likely a consequence of the fact that the forward shock still dominates the emission spectrum. Since this is tracing shock-heated CSM material, it reflects the composition of the CSM and not the composition of the inner ejecta. Thus, a lack of strong oxygen features should not be taken as any indication of the abundances in the SN ejecta as long as intermediate-width lines are still seen.

Another relevant detail concerns the line profiles. While SN 2005ip and SN 1988Z are otherwise very similar, they differ in that SN 2005ip shows asymmetric blueshifted line profiles, especially in its intermediate-width $H\alpha$ line at late times (Figure 1). The intermediate-width $H\alpha$ components of SN 1988Z remain much more symmetric at all epochs (Figure 2). This could signify a difference in dust-formation efficiency in the two SNe, or perhaps viewing-angle effects if the CSM interaction is not spherically symmetric (for example, SN 1988Z could be a ring or disk-like interaction seen pole-on, in which case dust cannot block emission from receding material). Interestingly, the late-time line profiles of SN 1998S, and to a somewhat lesser extent SN 1993J, do show blueshifted asymmetry that may be indicative of dust formation in these SNe. This was already discussed in detail for the case of SN 1998S by Mauerhan & Smith (2012). There have been no published studies of early-time spectropolarimetry of SN 1988Z or SN 2005ip, however.

3.4 Radio Emission from SN 2005ip

Very few radio SNe have been observed beyond 10 yr. Previous examples such as SNe 1986J, 1988Z, and 1995N (see, e.g., Van Dyk et al. 1993; Williams et al. 2002; Bietenholz et al. 2002; Chandra et al. 2009) were noted for having unusually luminous radio emission that peaked around 900 to 1100 days after the inferred explosion date. In Figure 7, we compare the 5 GHz radio luminosity observed toward SN 2005ip to these radio SNe observed at late times (1500–6000 days). SN 2005ip appears very similar in its radio luminosity to SN 1988Z at a comparable epoch, which is perhaps not surprising in light of the $H\alpha$ results above. The best fit to the observed radio light curve of SN 1988Z is based on a five-parameter model derived from Weiler et al. (1986):

$$S_\nu = K_1 \left(\frac{\nu}{5 \text{ GHz}} \right)^\alpha \left(\frac{t-t_0}{1 \text{ day}} \right)^\beta \left(\frac{1-e^{-\tau}}{\tau} \right), \quad (1)$$

$$\tau = K_2 \left(\frac{\nu}{5 \text{ GHz}} \right)^{-2.1} \left(\frac{t-t_0}{1 \text{ day}} \right)^\delta, \quad (2)$$

with $\alpha, \beta, \delta, K_1$, and K_2 as free parameters. The explosion date t_0 can be fixed from early-time optical photometry. In Williams et al. (2002), the fit parameters for the late-time (> 1500 day) light curve of SN 1988Z were $\alpha = -0.72$, $\beta = -2.73$, $\delta = -2.87$, $K_1 = 9.1 \times 10^8$, and $K_2 = 3.19 \times 10^8$. These parameters imply that the SN progenitor underwent mass loss of at least $1.2 \times 10^{-4} M_\odot \text{ yr}^{-1}$ for the last 10,000 yr before exploding. SN 2005ip is about 20% less luminous than SN 1988Z at 5 GHz and $t \approx 3750$ days, but it is a factor of a few more luminous in X-rays at the same epoch. Analysis of X-rays suggests significantly larger mass-loss rates of 10^{-3} to $10^{-2} M_\odot \text{ yr}^{-1}$ (Katsuda et al. 2014).

It is difficult to infer the physical parameters of the CSM surrounding SN 2005ip based on a single epoch of radio observations. However, given the similarity between SNe 2005ip and 1988Z at both optical and radio wavelengths, we can hypothesize that SN 2005ip has an extremely dense and clumpy CSM profile out to large radii. We plan to continue to monitor the radio and X-ray evolution of SN 2005ip in light of its recent $H\alpha$ brightening, and the results will be presented in a future paper.

3.5 Late-Time X-ray Emission

As noted in Section 2.3, the rate of fading of the X-ray luminosity of SN 2005ip implies a CSM density that falls off more steeply than for a steady wind with $\rho \propto r^{-s}$ and $s = 2$, which should yield a t^{-1} profile in the case of free-free emission from a wind. This would imply that the star’s mass-loss rate was ramping up in the last few thousand years of its life as it approached core collapse. This is qualitatively consistent with implications from the $H\alpha$ evolution noted above. The wind density being steeper than a steady wind is also consistent with the earlier analysis of X-rays by Katsuda et al. (2014). Looking at X-rays alone, the rate of fading appears to be consistent with a continuation of the trend inferred by Katsuda et al. (2014). This is interesting, since the $H\alpha$ luminosity shows a more sudden drop followed by a resurgence in recent data. It is possible that the coarse time sampling of the X-ray data has missed this peculiar variability, so future additional X-ray observations are required to resolve this.

Although the X-rays from SN 2005ip imply a CSM that falls off more steeply than a steady wind, it is interesting to note that the X-ray luminosity of SN 1988Z falls off even faster with time at a similar epoch after explosion than SN 2005ip (e.g., Figure 8

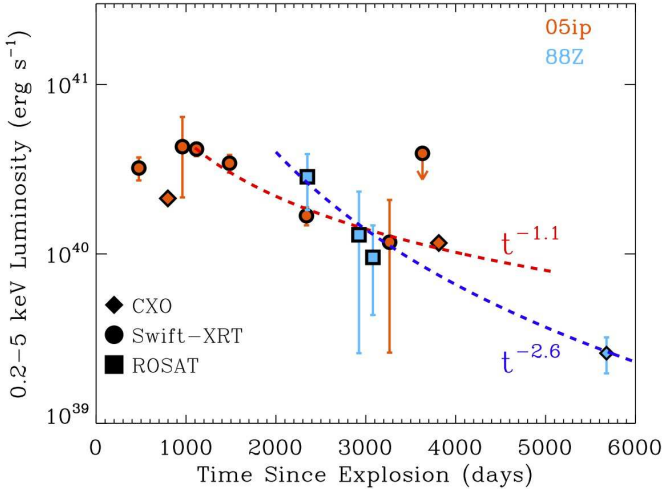


Figure 8. X-ray evolution of SN 2005ip (this paper) and SN 1988Z (Schlegel & Petre 2006). The X-ray luminosity plotted for SN 1988Z is a lower limit to the true luminosity of the transient, as no correction for any intrinsic neutral hydrogen column density was attempted by Schlegel & Petre (2006). For SN 1988Z Schlegel & Petre (2006) assumed a 5 keV plasma in collisional equilibrium. For comparison with this X-ray light curve of SN 1988Z, here we show the X-ray fluxes for SN 2005ip reduced in the same way (not corrected for intrinsic absorption, integrated over the same energy range of 0.5–2 keV). This is different from the data shown in Figure 3, but allows for a more direct comparison with SN 1988Z. The two SNe overlap in X-ray luminosity in this energy band, but have somewhat different decay rates.

and Schlegel & Petre 2006). Note that a direct comparison between X-rays from SN 2005ip and SN 1988Z is a bit tricky, because Schlegel & Petre (2006) made somewhat different assumptions in their analysis. Therefore, for the purpose of comparing the two objects in Fig 8, we have recalibrated our SN 2005ip X-ray data with the same assumptions (integrated over 0.5–2 keV, uncorrected for intrinsic absorption). Here we find that the X-ray luminosities are about the same at ~ 3000 d, although the somewhat faster decline of SN 2005ip is still apparent. Yet, despite this faster decline in X-rays around a decade after explosion, the $H\alpha$ luminosity of SN 1988Z then hit a plateau and did not decline for another decade after this epoch. This constant $H\alpha$ luminosity seems inconsistent with the steep drop in wind density implied by the X-rays. Overall, it seems that a clear lesson from comparing various diagnostics from different late-time interactors is that any single diagnostic by itself provides an incomplete picture, so readers should be aware that some of the corresponding mass-loss rate estimates are likely to be lower limits. Note that the value of \dot{M} that we derive from radio emission is an order of magnitude lower than from X-ray and $H\alpha$ observations of SN 2005ip at the same epoch.

Consider the comparison of SN 1988Z and SN 2005ip a decade after explosion. The two have roughly equal X-ray and $H\alpha$ luminosities, but SN 1988Z is more luminous in radio emission. A caveat is that the quoted X-ray luminosities are not bolometric X-ray luminosities, although we have tried to recalibrate our SN 2005ip X-ray data in the same way as had been done for SN 1988Z (Schlegel & Petre 2006). One might imagine that these inconsistencies could be attributed to some combination of clumping or aspherical geometry, which can influence the emissivity of $H\alpha$ or the escape of X-rays and radio differently for a given

CSM mass. Dense regions that emit strong $H\alpha$ emission might be self absorbed in the radio, for example, and a range of densities may exist simultaneously if the emitting region is clumpy. Katsuda et al. (2016) discussed how asymmetry might influence X-ray emission in SNe IIn. We noted earlier that there are some indications of asymmetry and different viewing angles between the two SNe (SN 2005ip shows asymmetric blueshifted line profiles in $H\alpha$ that imply dust formation blocks the far side, whereas SN 1988Z does not; this could perhaps be ascribed to a pole-on view of SN 1988Z and a nearly edge-on view of SN 2005ip). While such aspects are difficult to constrain with high confidence, the large binary fraction among massive stars (Moe & Di Stefano 2016; Sana et al. 2012; Chini et al. 2012; Kiminki & Kobulnicky 2012; Kiminki et al. 2012; Kobulnicky et al. 2014) and the high incidence of aspherical geometry in resolved CSM around nearby massive stars suggests that effects such as asymmetry and clumping may be the norm rather than an exception.

4 DISCUSSION

In this paper we have emphasized the remarkable similarity between the late-time evolution of SN 2005ip and that of SN 1988Z, which is the prototypical long-lived SN IIn. So far there are three main differences in their evolution.

First, the CSM interaction in SN 1988Z was stronger at early times and declined for the first 1000 days, whereas SN 2005ip had a more delayed onset of its strongest CSM interaction. SN 2005ip’s interaction remained roughly constant until day 1000, after which it tracked that of SN 1988Z. This relatively delayed onset in SN 2005ip was accompanied by stronger narrow coronal emission lines at early times, probably signifying a more highly clumped inner-wind region (compared to SN 1988Z), allowing the densest pre-shock regions to be photoionized by X-rays from a very fast blast wave (Smith et al. 2009a).

The second major difference is that SN 2005ip has just recently shown a drop and then a quick resurgence in its $H\alpha$ luminosity over the course of a few months, indicative of strong density fluctuations in its distant CSM. The recent sudden increase in $H\alpha$ would reflect a density increase by a factor of 2–5. SN 1988Z has shown no such behaviour, although brief blips cannot be ruled out by the coarse time sampling of our late-time SN 1988Z spectra. For a blast wave expanding at 2000–5000 km s $^{-1}$, fluctuations seen ~ 3500 days after SN 2005ip’s explosion would correspond to radii of $(0.6\text{--}1.5) \times 10^{17}$ cm, or roughly 0.02–0.05 pc from the star. Interestingly, this is consistent with the radius of a warm dust shell responsible for the near/mid-IR echo seen at early times (Fox et al. 2009, 2010), which was inferred to reside at ~ 0.03 pc from the star (Fox et al. 2011, 2013). This dust was ascribed to a shell of enhanced density at that location. It therefore seems likely that the sudden increase in the $H\alpha$ luminosity that we observe around day 3500 could in fact be caused by the forward shock reaching and overtaking this same dusty CSM shell. If so, continued study of this interaction may provide a novel way to investigate the destruction or survival of CSM dust that is hit by a SN blast wave.

Third, despite their similar $H\alpha$ luminosity evolution, SN 2005ip declines more slowly in X-rays than SN 1988Z, but it is also somewhat less luminous at radio wavelengths than SN 1988Z at a comparable epoch (see Sections 3.4 and 3.5 for details and caveats). This suggests that any one diagnostic taken alone gives an incomplete picture of the progenitor mass loss.

The recent $H\alpha$ variability suggests that SN 2005ip has strong

deviations from a monotonically decreasing wind density at large radii, but what caused this? A simple interpretation would be that changes in CSM density reflect previous changes in wind mass-loss rate. At a radius of 0.03 pc, and with a constant wind speed of $\sim 40 \text{ km s}^{-1}$ (somewhat faster wind speeds are appropriate for more luminous RSGs; see [Smith 2014](#)), this would point to substantial changes in mass loss about 1000 yr preceding core collapse. As noted in Section 1, sudden bursts of mass loss on these timescales before core collapse do not fall within the realm of currently suggested ideas that involve Ne and O burning, which are too brief for objects like SN 2005ip and SN 1988Z ([Quataert & Shiode 2012](#); [Shiode & Quataert 2014](#); [Smith & Arnett 2014](#)). Instead, it appears as if the mass-loss rate was ramping up in the last few thousand years before core collapse in SN 2005ip and SN 1988Z. Some evidence for such behaviour is observed among nearby populations of RSGs ([Beasor & Davies 2016](#)), and it may be expected theoretically ([Heger et al. 1997](#); [Yoon & Cantiello 2010](#); [Smith 2014](#)).

Although RSG winds may ramp up near the end of a star’s life, strong fluctuations in CSM density may point to episodic mass loss akin to eruptions of luminous blue variables (LBVs) or unsteady binary mass-transfer episodes. Indeed, LBV-like eruptive mass loss has been suggested as the possible origin of the CSM shells around SN 2005ip ([Fox et al. 2013](#); [Katsuda et al. 2014](#)). [Smith & Arnett \(2014\)](#) have discussed how binary interaction triggered by pre-SN evolution might instigate LBV-like mass loss through a rapid onset of common-envelope evolution. Recalling that LBVs are a phenomenological class and binary interaction is a physical mechanism, these might be two names for the same phenomenon. Some current ideas for LBVs do favour binary interaction as a necessary ingredient in their evolution ([Smith & Tombleson 2015](#)).

A drop in pre-shock density followed immediately by an increase in density, as indicated by the H α fluctuation of SN 2005ip, might also result from a temporary increase in wind speed that swept material into a thinner shell. Thus, variations in wind speed, as opposed to just wind mass-loss rate, might also give rise to such structures. Wind speeds could vary significantly if the progenitor experienced a blue loop on the Hertzsprung-Russell diagram, for example. Perhaps the common assumption of ballistic speeds is naive, but nevertheless, this material must be far from the star and quite old compared to the CSM overtaken by normal SNe II during their early bright phases.

Another puzzling aspect of SN 2005ip’s late-time behaviour concerns its X-ray emission. In 2013–2014, analysis of X-rays from SN 2005ip ([Katsuda et al. 2014](#)) indicated a drop in both the X-ray flux and the absorbing neutral H column density (N_{H}) along our line of sight (reaching the expected Galactic line-of-sight value by the last epoch). This prompted [Katsuda et al. \(2014\)](#) to suggest that SN 2005ip’s blast wave had reached the outer boundary of the dense shell. However, the similarity to SN 1988Z (which continued unabated for another decade after this epoch), the recent resurgence in H α emission from SN 2005ip, and strong radio and X-ray emission, indicate that its CSM interaction is not yet going away. In that case, how should we reconcile the observed drop in N_{H} ? [Katsuda et al. \(2014\)](#) considered the possibility that the outer RSG wind is ionized by the luminosity from CSM interaction, but found the ionization to be insufficient for expected shock parameters. However, they did not discuss the possibility of external influences on the RSG wind, and interpreted the drop in density as a shell resulting from a past LBV-like eruption, as noted above. (They also noted that a change in the degree of clumping might explain the drop in N_{H} .)

An alternative explanation for the origin of a sudden jump

in density at a large radius may be an otherwise normal steady wind that becomes confined by external pressure at large radii ([Garcia-Segura et al. 1996](#); [Chita et al. 2008](#); [Mackey et al. 2014](#)). If the progenitor was indeed a more massive star (above 18–20 M_{\odot}) so that it was an O-type star when on the main sequence, then its hot shocked main-sequence wind will provide an external pressure that might decelerate the RSG wind and confine it to a thin shell. (If the progenitor has similarly massive O-type neighbours in a young stellar cluster, the hot interior of the H II region might create the required external pressure and ionization.) [Mackey et al. \(2014\)](#) have discussed the interesting possibility that some SNe II may arise from the interaction between the SN shock and this type of externally confined, thin neutral shell. In practice, this may be quite rare: most normal RSG progenitors are at relatively low initial masses (i.e., 10–15 M_{\odot}), which means that they were not O-type stars on the main-sequence, and they reach the RSG phase long after associated O-type stars have died. On the other hand, more-massive RSGs that die sooner have much higher wind momentum in the RSG phase than assumed in the models, so it remains unclear if normal RSG winds are likely to yield SNe II through this process.

Although this scenario was proposed as a way to explain SNe II without appealing to eruptive pre-SN mass loss, it may also provide a way for an interacting SN to be “rejuvenated” in its old age, since the stalled shell is denser than a freely expanding wind. [Mackey et al. \(2014\)](#) estimate that such a shell can have its density enhanced by a factor of 80, and may contain a significant fraction (perhaps a third) of the total mass lost during the RSG phase. Their models demonstrate that a SN can show a bolometric luminosity spike at very late times from such a collision. In this case it is difficult to estimate the age of the shell, since its expansion may have stalled, and its radius depends on the external pressure as much as on the momentum of the RSG wind. Future monitoring of SN 2005ip may help to test this hypothesis, as the shock continues to make its way through this dense neutral shell and out into the ionized portion of the RSG wind, or if SN 2005ip resumes a very slow decline as SN 1988Z did. Also, higher-resolution spectra may be able to place tighter constraints on the pre-shock CSM expansion speed, since the narrow components are unresolved in our moderate-resolution spectra presented here.

Regardless of the true explanation for the density fluctuation in SN 2005ip’s outer CSM, it is useful to realize that mass-loss rates this high (several times 10^{-4} to $10^{-3} M_{\odot} \text{ yr}^{-1}$ or more) are quite extreme, and do not correspond to normal RSGs like Betelgeuse, where the wind is two orders of magnitude less dense ([Smith et al. 2009b](#)). The cool evolved stars with winds this dense are rare (see, e.g., [Smith 2014](#) for an overview of mass-loss rates), corresponding to the most luminous and extreme RSGs that are enshrouded by their own dusty winds, like VY CMa, NML Cyg, S Per, etc., or to self-enshrouded super-asymptotic giant branch (AGB) stars. In the cases of SN 1988Z and SN 2005ip, however, the very large CSM mass needed for their sustained high-luminosity CSM interaction has been estimated as 10 M_{\odot} or more. This confidently rules out super-AGB stars (total mass including a neutron star of only $\sim 8 M_{\odot}$) as their possible progenitors. This would be unlikely anyway, as these super-AGB stars that may undergo O-Ne-Mg core collapse in an electron-capture event are expected to produce a low SN kinetic energy of $\sim 10^{50}$ ergs ([Nomoto et al. 1982](#); [Nomoto 1987](#)). Thus, electron-capture SNe that produce SNe II through interaction may be expected to fade quickly (see, e.g., [Mauerhan et al. 2013](#)). SN 1988Z was hyperenergetic; up to day 3000, [Aretxaga et al. \(1999\)](#) estimate a total radiated energy for SN 1988Z of 10^{52} erg (model-dependent E_{rad}), and at least

2×10^{51} erg (observed E_{rad}). SN 2005ip appears very similar in many respects, and is even more luminous and slower to decline in X-rays.

The extreme RSGs mentioned have initial masses of order 25–35 M_{\odot} , higher than normal unobscured RSGs, with more tightly bound cores that may require more energetic explosions than normal SNe II-P. This reinforces earlier suggestions that these extreme RSGs (as opposed to normal RSGs) are the likely progenitors of some SNe IIn, including long-lived SN 1988Z-like events (Smith et al. 2009a,b; Van Dyk et al. 1993; Williams et al. 2002). More massive LBV stars may also be able to supply the required amount of CSM mass (Smith 2014; Smith & Owocki 2006). However, the steady late-time decline over decades in the case of SN 1988Z argues in favour of a freely expanding, slow, and sustained dense RSG wind, rather than the sporadic eruptive mass loss characteristic of LBVs. For SN 2005ip, future observations of its continuing evolution through the extended CSM may help us choose more confidently between an extreme RSG — perhaps exposed to external ionizing radiation from its environment — or an eruptive progenitor. In any case, the strong variability in $H\alpha$ around day 3500 in SN 2005ip has not been seen so clearly before at such late times in SNe IIn, and suggests that similar late-time observations of other objects can provide important constraints on the variability in their pre-SN mass loss.

Strong and variable mass loss of the type seen here occurring 1000 yr before death presents a challenge for models of pre-SN evolution. Once we have a larger number of known SNe IIn with such enduring strong CSM interaction, it would be interesting to investigate their statistical proximity to H II regions as compared to other populations of SNe.

ACKNOWLEDGMENTS

We thank an anonymous referee for helpful suggestions. Support was provided by the National Science Foundation (NSF) through grants AST-1210599 and AST-1312221 to the University of Arizona. C.D.K.'s research receives support from NASA through Contract Number 1255094 issued by JPL/Caltech. W.F. was supported by NASA through an Einstein Postdoctoral Fellowship. The supernova research of A.V.F.'s group at U.C. Berkeley is supported by Gary & Cynthia Bengier, the Richard & Rhoda Goldman Fund, the Christopher R. Redlich Fund, the TABASGO Foundation, and NSF grant AST-1211916.

We thank the staffs at the MMT and Keck Observatories for their assistance with the observations. Observations using Steward Observatory facilities were obtained as part of the large observing program AZTEC: Arizona Transient Exploration and Characterization. Some of the observations reported in this paper were obtained at the MMT Observatory, a joint facility of the University of Arizona and the Smithsonian Institution. This research was also based in part on observations made with the LBT. The LBT is an international collaboration among institutions in the United States, Italy, and Germany. The LBT Corporation partners are the University of Arizona on behalf of the Arizona university system; the Istituto Nazionale di Astrofisica, Italy; the LBT Beteiligungsgesellschaft, Germany, representing the Max-Planck Society, the Astrophysical Institute Potsdam, and Heidelberg University; the Ohio State University and the Research Corporation, on behalf of the University of Notre Dame, University of Minnesota, and University of Virginia. Some of the data presented herein were obtained at the W.M. Keck Observatory, which is operated as a scientific partnership among the California Institute of Technology, the University of California, and NASA; the observatory was made possible by the generous financial support of the W.M. Keck Foundation. The authors wish to recognize and acknowledge the very significant cultural role and reverence that the summit of Mauna Kea has always had within the indigenous Hawaiian community. We are most fortunate to have the opportunity to conduct observations from this mountain.

REFERENCES

- Andrews JE, Smith N, Mauerhan JC, 2015, MNRAS, 451, 1413
 Aretxaga I, et al. 1999, MNRAS, 309, 343
 Asplund M, Grevesse N, Sauval AJ, Scott P, 2009, ARA&A, 47, 481
 Barlow MJ, et al., 2005, ApJ, 627, L113
 Beasor ER, Davies B, 2016, MNRAS, in press (arXiv:1608.03895)
 Bietenholz MF, Bartel N, Rupen MP, 2002, ApJ, 581, 1132
 Burrows DN, et al., 2005, SSR, 120, 165
 Byard PL, O'Brien TP, 2000, Proc. SPIE, 4008, 934
 Chandra P, et al., 2009, ApJ, 690, 1839
 Chevalier RA, Fransson C, 1994, ApJ, 420, 268
 Chini R., Hoffmeister V. H., Nasserri A., Stahl O., Zinnecker H., 2012, MNRAS, 424, 1925
 Chita SM, Langer N, van Marle AJ, Garca-Segura G, Heger A, 2008, A&A, 488, L37
 Chugai NN, Chevalier RA, 2006, ApJ, 641, 1051
 Chugai NN, Danziger IJ, 1994, MNRAS, 268, 173
 Crotts APS, Heathcote SR, 2000, ApJ, 528, 426
 Dessart L, Audi E, Hillier DJ 2015, MNRAS, 449, 4304
 Faber SM, et al., 2003, in Iye M, Moorwood AFM, ed., Proc. SPIE Vol. 4841, Instrument Design and Performance for Optical/Infrared Ground-based Telescopes. SPIE, Bellingham, p. 1657
 Fabian AC, Terlevich R, 1996, MNRAS, 280, L5
 Fassia A, et al., 2001, MNRAS, 325, 907
 Filippenko AV, 1991, in SN 1987A and Other Supernovae, ed. IJ Danziger & K Kjar (Garching: ESO), 343
 Filippenko AV, 1997, ARAA, 35, 309
 Fransson C, et al., 1996, ApJ, 461, 993
 Fransson C, Björnsson C-I, 1998, ApJ, 509, 861
 Fransson C, et al. 2014, ApJ, 797, 118
 Fox OD, et al., 2009, ApJ, 691, 650
 Fox OD, Chevalier RA, Dwek E, Skrutskie MF, Sugerman BEK, Leisenring JM, 2010, ApJ, 725, 1768
 Fox OD, Chevalier RA, Skrutskie MF, Soderberg AM, Filippenko AV, Ganeshalingam M, Silverman JM, Smith N, Steele TN, 2011, ApJ, 741, 7
 Fox OD, et al., 2013, AJ, 146, 2
 Fox OD, et al., 2015, MNRAS, 454, 4366
 France K, et al., 2015, ApJ, 801, L16
 Gal-Yam A, et al., 2014, Nature, 509, 471
 Garca-Segura G, Langer N, Mac Low MM, 1996, A&A, 316, 133
 Gehrels N, et al., 2004, ApJ, 611, 1005
 Greisen EW, 2003, Information Handling in Astronomy — Historical Vistas, 285, 109
 Heger A, Jeannin L, Langer N, Baraffe I, 1997, A&A, 327, 224
 Katsuda S, Maeda K, Nozawa T, Pooley D, Immler S, 2014, ApJ, 780, 184
 Katsuda S, et al. 2016, arXiv:1609.09093
 Kelson D, 2003, PASP, 115, 688
 Khasov D, et al., 2016, ApJ, 818, 3
 Kiewe M, et al., 2012, ApJ, 744, 10
 Kiminki D.C., Kobulnicky H.A., 2012, ApJ, 751, 4
 Kiminki D.C. et al. 2012, ApJ, 747, 41
 Kobulnicky H.A. et al., 2014, ApJS, 213, 34
 Leonard DC, et al., 2000, ApJ, 536, 239
 Li W, et al., 2011, MNRAS, 412, 1441
 Mackey J, Mohamed S, Gvaramadze VV, Kotak R, Langer N, Meyer DMA, Moriya TJ, Neilsen HR, 2014, Nature, 512, 282
 Margutti R, et al., 2013, MNRAS, 428, 729
 Margutti R, et al., 2016, preprint
 Matheson T, et al., 2000, AJ, 120, 1499
 Mauerhan J, Smith N, 2012, MNRAS, 424, 2659
 Mauerhan JC, Smith N, Silverman JM, et al., 2013, MNRAS, 431, 2599
 Meaburn J, Bryce M, Holloway AJ, 1995, A&A, 229, L1
 Michael E, McCray R, Borkowski KJ, Pun CSJ, Sonneborn G, 1998, ApJ, 492, L143
 Miller AA, et al., 2010a, MNRAS, 404, 305

- Miller AA, Smith N, Bloom JS, Chornock R, Filippenko AV, Prochaska JX, 2010b, *AJ*, 139, 2218
- Milisaavljevic D, Fesen RA, Chevalier RA, Kirshner RP, Challis P, Turatto M, 2012, *ApJ*, 751, 25
- Milisaavljevic D, et al., 2015, *ApJ*, 815, 120
- Moe M, Di Stefano R, 2016, preprint (arXiv:1606.05347)
- Niemela VS, Ruiz MT, Phillips MM. 1985, *ApJ*, 289, 52
- Nomoto K, 1987, *ApJ*, 277, 791
- Nomoto K, Sugimoto D, Sparks WM, Fesen RA, Gull TR, Miyaji S, 1982, *Nature*, 299, 803
- Ofek EO, et al., 2014, *ApJ*, 781, 42
- Oke JB, Cohen JG, Carr M, et al., 1995, *PASP*, 107, 375
- Pozzo M, et al., 2004, *MNRAS*, 352, 457
- Quataert E, Shiode J, 2012, *MNRAS*, 423, L92
- Quimby R, Wheeler JC, Hoflich P, Akerlof CW, Brown PJ, Rykoff ES. 2007, *ApJ*, 666, 1093
- Sana H, de Mink SE, de Koter A, et al., 2012, *Science*, 337, 444
- Schlegel EM, Petre R, 2006, *ApJ*, 646, 378
- Shiode J, Quataert E, 2014, *ApJ*, 780, 96
- Shivvers I, Mauerhan JC, Leonard DC, Filippenko AV, Fox OD, 2015, *ApJ*, 806, 213
- Smith N, 2014, *ARA&A*, 52, 487
- Smith N, Arnett WD, 2014, *ApJ*, 785, 82
- Smith N, Owocki SP, 2006, *ApJ*, 645, L45
- Smith N, Tombleson R, 2015, *MNRAS*, 447, 602
- Smith N, Li W, Foley RJ, et al., 2007, *ApJ*, 666, 1116
- Smith N, Chornock R, Li W, Ganeshalingam M, Silverman JM, Foley RJ, Filippenko AV, Barth AJ, 2008a, *ApJ*, 686, 467
- Smith N, et al., 2008b, *ApJ*, 686, 485
- Smith N, et al., 2009a, *ApJ*, 695, 1334
- Smith N, Hinkle KH, Ryde N, 2009b, *AJ*, 137, 3558
- Smith N, et al., 2010, *ApJ*, 709, 856
- Smith N, et al., 2011, *MNRAS*, 412, 1522
- Smith N, et al., 2012, *AJ*, 143, 17
- Smith N, et al., 2015, *MNRAS*, 449, 1876
- Sonneborn G, et al., 1998, *ApJ*, 492, L139
- Stathakis RA, Sadler EM, 1991, *MNRAS*, 250, 786
- Stritzinger M, et al., 2012, *ApJ*, 756, 173
- Taddia F, et al., 2013, *A&A*, 38, 113
- Turatto M, et al., 1993, *MNRAS*, 262, 128
- Van Dyk SD, Weiler KW, Sramek RA, Panagia N 1986, *ApJ*, 419, L69
- Weiler KW, Sramek RA, Panagia N, van der Hulst JM, Salvati M, 1986, *ApJ*, 301, 790
- Weiler KW, Panagia N, Montes MJ, Sramek RA. 2002, *ARA&A*, 40, 387
- Williams CL, Panagia N, Van Dyk SD, Lacey CK, Weiler KW, Sramek RA, 2002, *ApJ*, 581, 396
- Woosley SE, 2016, preprint (arXiv:1608.08939)
- Woosley SE, Blinnikov S, Heger A, 2007, *Nature*, 450, 390
- Wright EL, 1980, *ApJ*, 242, L23
- Yoon SC, Cantiello M, 2010, *ApJ*, 717, L62

This figure "fig8.jpg" is available in "jpg" format from:

<http://arxiv.org/ps/1612.02011v1>